Acta Crystallographica Section D
Biological Crystallography
ISSN 0907-4449

Regulation of catalytic function by molecular association: structure of phospholipase A_2 from *Daboia russelli pulchella* ($DPLA_2$) at 1.9 Å resolution

Vikas Chandra,[a] Punit Kaur,[a] Jayasankar Jasti,[a] Ch. Betzel[b] and T. P. Singh[a]*

[a]Department of Biophysics, All India Institute of Medical Sciences, New Delhi 110029, India, and [b]Institute of Medical Biochemistry and Molecular Biology, UKE, c/o DESY, Notkestrasse 85, 22603, Hamburg, Germany

Correspondence e-mail: tps@aiims.aiims.ac.in

Received 6 June 2001
Accepted 6 September 2001

PDB Reference: phospholipase A_2, 1fb2.

The crystal structure of phospholipase A_2 from the venom of *Daboia russelli pulchella* has been refined to an *R* factor of 0.216 using 17 922 reflections to 1.9 Å resolution. The structure contains two crystallographically independent molecules in the asymmetric unit. The overall conformations of the two molecules are essentially the same except for three regions, namely the calcium-binding loop including Trp31, the β-wing and the C-terminal residues 119–131. Although these differences have apparently been caused by molecular packing, they seem to have functional relevance. Particularly noteworthy is the conformation of Trp31, which is favourable for substrate binding in one molecule as it is aligned with one of the side walls of the hydrophobic channel, whereas in the other molecule it is located at the mouth of the channel, thereby blocking the entry of substrates leading to loss of activity. This feature is unique to the present structure and does not occur in the dimers and trimers of other PLA_2s.

1. Introduction

Phospholipase A_2 (PLA_2; E.C. 3.1.1.4) is a major component of snake venoms and induces more than one pharmacological effect in animals. PLA_2s are broadly divided into two structural groups: class I, similar to pancreatic PLA_2, are typically found in elapid venoms, whereas class II PLA_2s are usually found in the crotalid and viperid venoms. *Daboia russelli* or Russell's viper is a class II PLA_2 and contains at least four subspecies according to its geographic origin: *D. russelli formosensis* (Taiwan), *D. russelli pulchella* (Sri Lanka and South India), *D. russelli russelli* (North India and Pakistan) and *D. russelli siamensis* (China and southeast Asia) (Jayanthi & Gowda, 1988; Woodhams *et al.*, 1990; Tsai *et al.*, 1996).

PLA_2 specifically hydrolyzes the 2-acyl ester bond of 1,2-diacyl-3-*sn*-phospholipids (van Deenen & de Haas, 1963). The enzyme catalyzes reactions at a lipid–aqueous interface and the phospholipase activity is much higher on aggregated substrates such as monolayers, bilayers, micelles, membranes and vesicles than on monomolecular dispersed soluble substrates (Yuan *et al.*, 1990). This phenomenon has been termed 'interfacial catalysis' and includes interfacial binding of the enzyme and 'activation steps' (Scott *et al.*, 1990). Structural changes were observed in PLA_2 upon its binding to membranes and were thought to be a prerequisite for enzyme activation (Tatulian *et al.*, 1997). Thus, it is evident that modulation of membrane-associated PLA_2 activity will influence cellular functions such as chemostatis, cytotoxicity and cell differentiation. It has also been established that the interfacial absorption of PLA_2 on membrane is driven by

electrostatic forces (Scott *et al.*, 1994). Electrostatic interactions between the positive charges of the PLA_2 recognition site and the negatively charged anionic head groups of phospholipids optimize the catalysis and are important for the adsorption and orientation of the enzyme at the lipid–water interface.

The roles of structural changes in PLA_2 upon its binding to membranes and the substrate-induced enzyme aggregation in PLA_2 catalysis have not yet been clearly understood. In an attempt to provide a firm basis for structure-based PLA_2 catalysis, we report here the three-dimensional structure of PLA_2 from *D. russelli pulchella* ($DPLA_2$) at 1.9 Å resolution with two molecules in the crystallographic asymmetric unit. The low-resolution structure of $DPLA_2$ was reported previously (Chandra *et al.*, 2000). The present high-resolution analysis provides additional information, particularly on the dimerization interface involving the two crystallographically independent molecules in the structure and the specific differences between the two molecules.

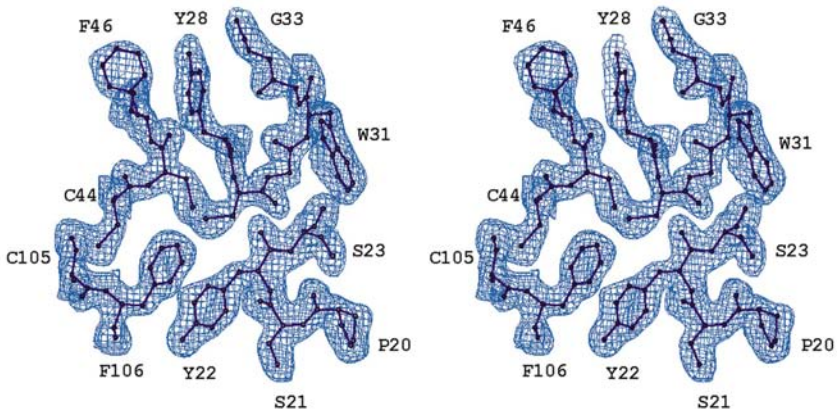

Figure 1
A region of the final $2F_o - F_c$ electron-density map contoured at 1.5σ and the corresponding refined model. The diagram was produced using the program *O* (Jones *et al.*, 1991).

2. Experimental

2.1. Purification and crystallization of $DPLA_2$

Crude venom containing $DPLA_2$ was obtained from Irula cooperative snake farm, Tamilnadu, India. The purification was carried out as described previously (Chandra *et al.*, 1999). Pure $DPLA_2$ was crystallized by the hanging-drop vapour-diffusion method using a 15 mg ml^{-1} concentration of protein in 20 m*M* sodium cacodylate buffer pH 6.5. It was equilibrated against 1.4 *M* ammonium sulfate in the presence of 3% dioxane. Very stable rectangular crystals of dimensions up to $0.4 \times 0.3 \times 0.2$ mm were obtained at 298 K within two weeks.

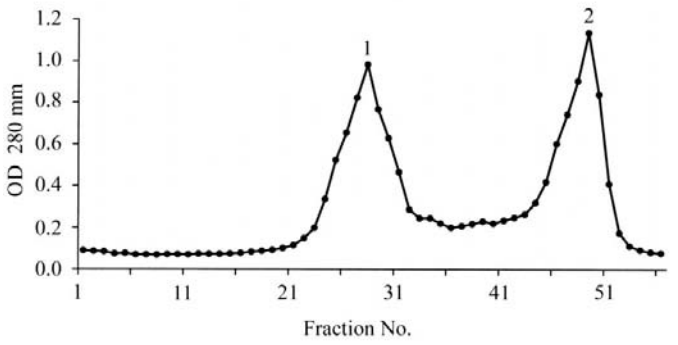

Figure 2
Gel-filtration profile of the mixture of $DPLA_2$ and lysozyme using a Sephadex G-50 column (100×1.6 cm). Peak 1 corresponds to $DPLA_2$ and peak 2 corresponds to lysozyme.

2.2. Data collection

The crystals diffracted to 1.9 Å resolution. The data were collected on EMBL beamline X-11 at DESY, Hamburg with $\lambda = 0.98$ Å using a MAR345 imaging-plate scanner with 1.0° rotation for each image. A single crystal was mounted in a nylon loop and flash-frozen in a nitrogen stream at 100 K using 15% glycerol as a cryoprotectant while maintaining the ionic strength of the precipitant. The data were processed using the *DENZO* and *SCALEPACK* program packages (Otwinowski, 1993; Minor, 1993). The results of data collection and processing are given in Table 1. The data indicated a large mosaicity of 0.7°, presumably a consequence of freezing. The unit-cell parameters of the crystals were found to be slightly different from those reported earlier (Chandra *et al.*, 2000). This could also be a consequence of the use of cryocooling in this study.

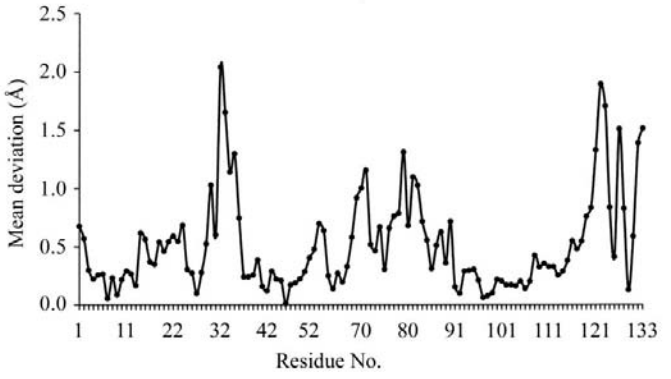

Figure 3
Deviations of C^{α} positions on superposition of molecules *A* and *B* against residue numbers.

2.3. Refinement

The starting model was the structure of $DPLA_2$ previously determined at 2.4 Å resolution by the molecular-replacement method (Chandra *et al.*, 2000), which was refined using the simulated-annealing method of the program *X-PLOR* (Brünger, 1992*a*) to an *R* factor of 18.8% in the resolution

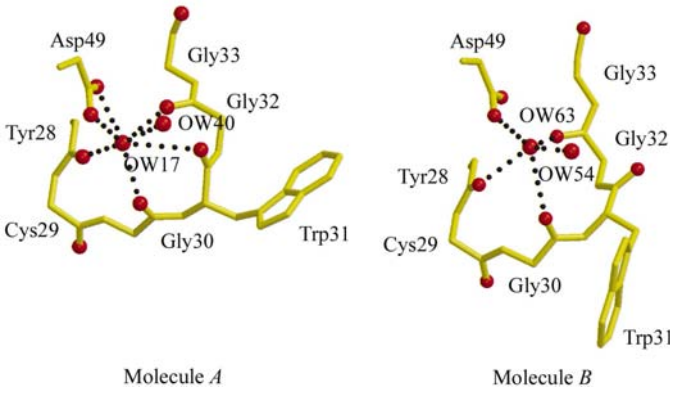

Figure 4
The calcium-binding loop in the two molecules. A water molecule is observed at the site of calcium ion in each molecule. The conformation of Trp31 in molecule *A* is clearly different in the two molecules.

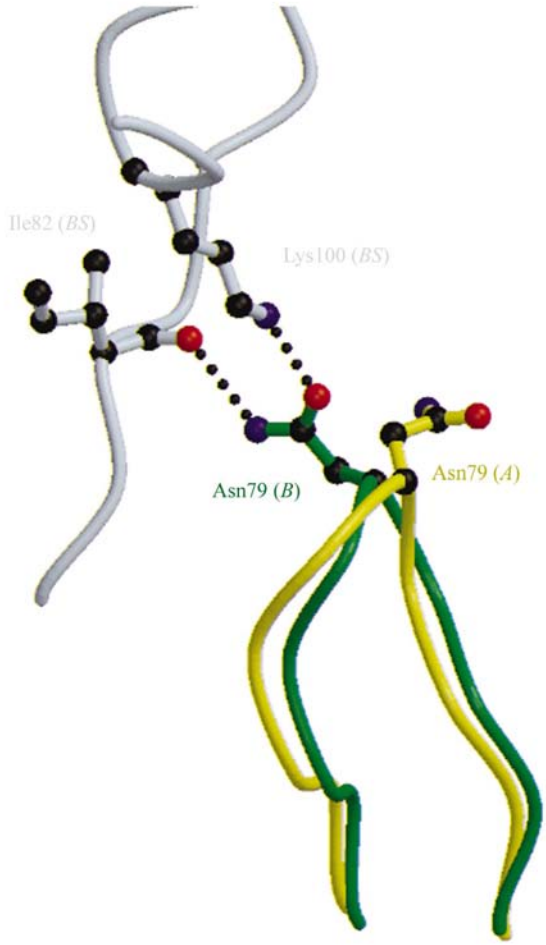

Figure 5
Superposition of β-wings of molecules *A* and *B*. The side chain of Asn79 of molecule *B* interacts with Ile82 and Lys100 of a symmetry-related molecule *B*. The corresponding interactions are absent in molecule *A*, in which the side chain of Asn79 is exposed to solvent. *BS* indicates a symmetry-related *B* molecule.

range 20.0–2.4 Å. Here, the new 1.9 Å data set was used for extension of the resolution and improvement of the structure. In the first step, refinement was carried out with the program *X-PLOR*. In each step, $2F_o - F_c$ and $F_o - F_c$ maps were calculated to improve the structures in the density maps using the program *O* (Jones *et al.*, 1991). The 2.4 Å model without solvent molecules was used as the starting point. The resolution was extended stepwise to 2.3, 2.2, 2.1, 2.0 and 1.9 Å. In the 1.9 Å refinement step, water molecules were temporarily picked up from the $F_o - F_c$ electron-density map contoured at 3σ level. Upon refinement, water molecules were rejected if they moved beyond the hydrogen-bond distance. At the end of the refinement using *X-PLOR*, the model contained 1888 atoms corresponding to 242 amino acids from two crystallographically independent molecules and 213 water molecules. This model was further refined using the program *CNS* (Brünger *et al.*, 1990, 1998; Brünger, 1992*b*) in the same resolution range. In this refinement, the side chains of 17 residues were found to be discrete rotamers from inspection of both $2F_o - F_c$ and $F_o - F_c$ maps. The split side chains of these residues were refined with an occupancy of 0.5, which was estimated from electron densities. The temperature factors of water O atoms were in general lower than 40.0 Å^2, with a maximum value of 88.7 Å^2. All the water molecules were refined with unit occupancies and variable temperature factors. A final *R* factor of 21.6% and free *R* factor of 27.2% were obtained in the resolution range 20.0–1.9 Å (Table 2).

3. Results and discussion

3.1. Quality of the model

The final model consists of 1888 protein atoms from 242 amino-acid residues and 213 water molecules. The protein molecules have a geometry close to ideal, with r.m.s. deviations of 0.006 Å and 1.3° from standard values for bond lengths and angles, respectively. 87% of the residues were found in the most favoured regions of the Ramachandran plot (Ramachandran & Sasisekaran, 1968), while no residues were present in the disallowed regions. The mean deviation of

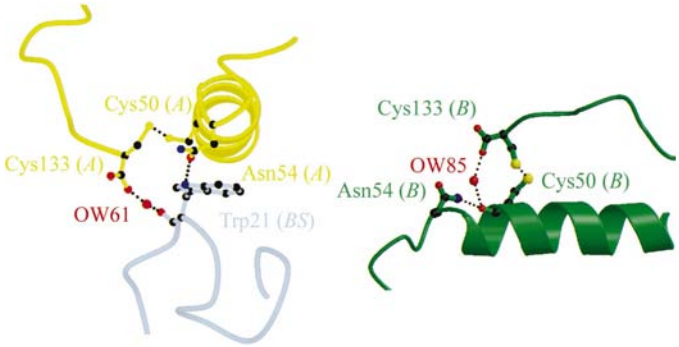

Figure 6
Interactions of the C-terminal Cys133. In addition to the intramolecular disulfide linkage with Cys50 it interacts intramolecularly in molecule *B* and intermolecularly in molecule *A*. *BS* indicates a symmetry-related *B* molecule.

Table 1
Overall statistics of data processing.

Values in parentheses refer to the highest resolution shell (2.0–1.9 Å).

Space group	$C222_1$
Unit-cell parameters (Å)	a = 76.10, b = 88.05, c = 79.37
Resolution range (Å)	20.0–1.9
No. of unique reflections	17922
Completeness (20.0–1.9 Å) (%)	91.0 (99.0)
Redundancy	4.1
R_{sym} (%)	2.6 (16.3)
Mean $I/\sigma(I)$	12.6 (5.6)
V_M (Å^3 Da^{-1})	2.62
Solvent content (%)	53.0
Z (No. of molecules in the unit cell)	16

Table 2
Summary of crystallographic refinement.

Refinement	
Resolution limits (Å)	20.0–1.9
No. of reflections	17922
Working set	17059
Test set (5%)	863
R factor (%)	21.6
Free R factor (%)	27.2
Model	
Protein atoms	1888
Water molecules	213
R.m.s. deviations from ideal values	
Bond lengths (Å)	0.006
Bond angles (°)	1.3
Dihedral angles (°)	23.1
Overall G factor	0.20
Average B factors (Å^2)	
Main-chain atoms	41.8
Side-chain atoms	43.6
All protein atoms	42.7
Solvent molecules	51.0

coordinates in the final model estimated from a Luzzati plot (Luzzati, 1952) was found to be in the range 0.24–0.29 Å (data not shown). All residues fitted the electron density exceptionally well in the refined structure (Fig. 1). The refinement statistics are given in Table 2.

3.2. Molecular association

The structure contains two crystallographically independent molecules *A* and *B* in the asymmetric unit. The molecules are associated through a broad interface between them. They form two strong intermolecular direct hydrogen bonds and a number of hydrogen bonds through water molecules. In addition, several hydrophobic interactions have also been observed between them. Thus, the association of the two molecules in $DPLA_2$ is strong and presents a unique feature of molecular association. The two molecules were found to exist in association even in solution. The gel-filtration profile of the mixture of $DPLA_2$ and lysozyme using a Sephadex G-50 column (100.0 × 1.6 cm) is shown in Fig. 2. The activity data indicates that peak 1 corresponds to $DPLA_2$ and peak 2 belongs to lysozyme. Also, the estimation of molecular weights of peaks 1 and 2 using void volume approximations are 28 and 14 kDa, respectively. The molecular weight of 28 kDa for peak 1 corresponds to the molecular weights of two $DPLA_2$ molecules.

The overall conformations of the two molecules are similar. The superimposition of molecule *A* on *B* shows an r.m.s. deviation of 0.69 Å for the C^α atoms. A plot of the deviation of the C^α positions of molecules *A* and *B* against residue number is shown in Fig. 3. There are three important regions which show subtle differences in the conformations of the two molecules. These are the calcium-binding loop including Trp31 (residue 25–34), the β-wing consisting of two antiparallel β-stands in the stretch residues 74–85 and residues 119–131. These regions are functionally important and are located at the molecular surface where conformational variability is more pronounced. Similar results were obtained in the recently determined structure of bovine pancreatic phospholipase A_2 carried out at 0.97 Å resolution (Steiner *et al.*, 2001).

3.3. Calcium-binding loop

The calcium-binding loop extends from Tyr25 to Gly33. The presence of two half cysteines and four glycine residues suggests a specially conformed backbone underlying an important function. In the present structure, calcium is not present but the calcium-binding site is occupied by a water molecule in each molecule. As seen from Fig. 4, the interactions of water with the loop and Asp49 in molecules *A* and *B* differ considerably. In molecule *A*, water is at hydrogen-bonding distances from the four carbonyl O atoms of Tyr28, Gly30, Trp31 and Gly32, the two carboxyl O atoms $O^{\delta1}$ and $O^{\delta2}$ of Asp49, and a water molecule OW40. The temperature factor of this water molecule for occupancy 1 is 25 Å^2. On the other hand, in molecule *B* there are only five such distances involving the backbone O atoms of Tyr28, Gly30 and Gly32, one O atom $O^{\delta2}$ from the carboxyl group of Asp49 and one water molecule OW54. The temperature factor for this water molecule is 45 Å^2. Despite this, the average temperature for the atoms of the calcium-binding loop in molecule *A* is 40 Å^2, which is more than that in molecule *B* (36 Å^2), indicating the effect of other forces that might be responsible for the stabilization and flexibility of the calcium-binding loops in the two molecules. For example, Trp31 of molecule *B* adopts the conformation with a χ^1 angle of -76.5° in order to form an intermolecular hydrogen bond through its N^ε with Asn54 $O^{\delta2}$. On the other hand, the side chain of Trp31 of molecule *A* adopts a conformation with a χ^1 torsion angle of -179.6° and protrudes into the interstitial solvent channels in the crystals. This conformation in molecule *A* leads to an arrangement in which the backbone O atom of Trp31 in molecule *A* points towards the interior of the loop while the corresponding O atom in molecule *B* is placed facing outward. Thus, the side chains of Trp31 in molecules *A* and *B* are disposed in opposite directions. Owing to the proximity of the Trp31 side chain to the hydrophobic channel, its conformation has a direct influence on the binding of substrates and inhibitors to PLA_2.

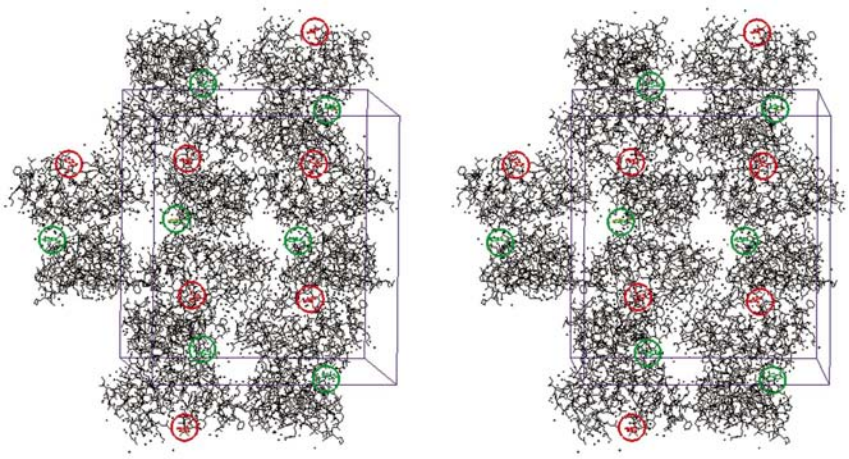

Figure 7
Stereo drawing of the packing of molecules in the unit cell. Trp31 is located at the mouth of the substrate-binding channel. The red circles show the position of Trp31 in molecule *B*, while the green ones indicate that of molecule *A*. Green circles containing Trp31 (*A*) are exposed to the solvent while red circles containing Trp31 (*B*) are completely blocked by molecular packing.

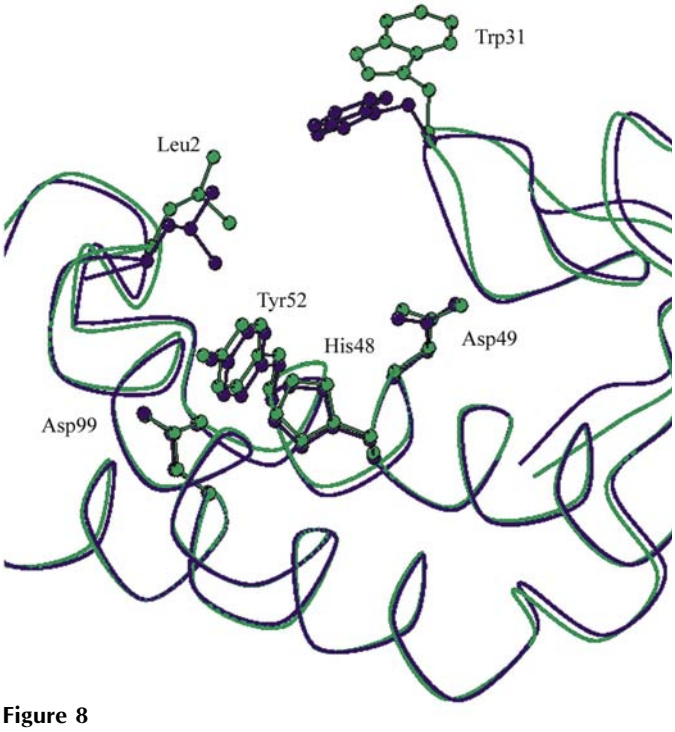

Figure 8
Positioning of Trp31 *vis-à-vis* the hydrophobic binding channel. The placement of Trp31 in molecule *B* (blue) reduces the width of the channel, thus impairing its binding capability while the corresponding width in molecule *A* (green) is optimum. The distances between the two nearest atoms of Leu2 and Trp31 are 8.3 and 4.7 Å in molecules *A* and *B*, respectively.

3.4. β-Wing

The chain segment containing residues 75–84 protrudes out of the core of the molecule and forms an antiparallel β-sheet. The two β-sheets containing residues 75–78 and 81–84 are held by a tight β-turn of type I′ conformation (Venkatachalam, 1968) involving residues 78–81. The β-wings in two molecules are differently oriented. The β-turn in molecule *B* is considerably distorted, leading to a different orientation of the side chains of Asn79 (Fig. 5). This seems to have been caused by intermolecular interactions of Asn79 of molecule *B* through $N^{\delta1}$ and $O^{\delta2}$ with Ile82 CO and Lys100 N^{ε} of a symmetry-related molecule. In molecule *A*, the side chain of Asn79 points towards the solvent. These differences, although apparently associated with the packing of the molecules in the crystalline state, are linked to a specific function.

3.5. C-terminal region

The C-terminal segment (Leu119–Cys133) adopts an extended conformation in both molecules. However, the conformations of the molecules differ substantially, even though the C-terminal residue Cys133 is linked to Cys50 through a disulfide bridge which is conserved in all group II PLA_2s. One of the carboxy-terminal O atoms of Cys133 of molecule *B* forms an intramolecular bridge *via* a water molecule OW85 with the CO of its disulfide-bridge partner Cys50, whereas Cys133 of molecule *A* is involved in an intermolecular interaction with the CO of a symmetry-related Trp31 (*B*) (Fig. 6).

3.6. Molecular packing and structural changes

The PLA_2 molecules tend to associate at high concentrations and exist as dimers (Keith *et al.*, 1981; Perbandt *et al.*, 1997) and trimers (Segelke *et al.*, 1998). The same is true of $DPLA_2$. As described earlier, the differences between the two molecules involve the crucial Trp31, the β-wing and the C-terminal region. The changes in Trp31 and the C-terminal region are interlinked through the intermolecular water bridge between Cys133 O and Trp31 O of a symmetry-related molecule *B*.

It is noteworthy that Trp31 and Asn79 of molecule *B* are involved in strong intermolecular interactions while the corresponding parts of molecule *A* are exposed to solvent (Fig. 7). Unlike the formations of dimers and trimers in other PLA_2 structures where the hydrophobic channels are shielded by each other, the association of two crystallographically independent molecules in the present structure places them back to back in such a way that the binding surfaces are fully accessible. However, the pairs of two crystallographically independent molecules are packed in such a manner in the crystalline state that the entry to the putative catalytic site of molecule *B* is blocked by other symmetry-related molecules. However, the hydrophobic channel of molecule *A* opens into the solvent region, making it accessible to substrates and inhibitors (Fig. 7). In addition, the conformations of Trp31 in molecules *A* and *B* differ drastically owing to the involvement of Trp31 in the strong intramolecular interactions in *A* and intermolecular forces in *B*. Futhermore, the side chain of

Trp31 in *A* moves away from the binding surface, leaving it wide open for easy diffusion of the substrate (Fig. 8). On the other hand, the intermolecular interactions involving Trp31 of molecule *B* induce its side chain to adopt a conformation in which the mouth of the binding channel is hindered by the side chain of Trp31 (Fig. 8). The shortest distance between any two atoms from the Trp31 side chain and that on the opposite wall of the hydrophobic channel is 4.7 Å in molecule *B* and 8.3 Å in molecule *A*. Therefore, it may be concluded that the binding site in molecule *A* is accessible while it is completely blocked in molecule *B*. This is a significant finding and explains the observations of lower activities in certain PLA_2s owing to molecular associations.

This work was supported by a grant from Department of Science and Technology, New Delhi, India.

References

Brünger, A. T. (1992*a*). *X-PLOR v3.1 User's Guide.* New Haven, Connecticut, USA: Yale University Press.

Brünger, A. T. (1992*b*). *Nature (London)*, **355**, 472–474.

Brunger, A. T., Adams, P. D., Clore, G. M., Delano, W. L., Gros, P., Grosse-Kunstleve, R. W., Jiang, J. S., Kuszewski, J., Nilges, N., Pannu, N. S., Read, R. J., Rice, L. M., Simonson, T. & Warren, G. L. (1998). *Acta Cryst.* D**54**, 905–921.

Brünger, A. T., Krukowski, A. & Erickson, J. (1990). *Acta Cryst.* A**46**, 585–593.

Chandra, V., Kaur, P., Srinivasan, A. & Singh, T. P. (2000). *J. Mol. Biol.* **296**, 1117–1126.

Chandra, V., Nagpal, A., Srinivasan, A. & Singh, T. P. (1999). *Acta Cryst.* D**55**, 925–926.

Deenen, L. L. M. van & de Haas, G. H. (1963). *Biochim. Biophys. Acta*, **70**, 538–553.

Jayanthi, G. P. & Gowda, T. V. (1988). *Toxicon*, **26**, 257–264.

Jones, T. A., Zou, J., Cowan, S. W. & Kjeldgaard, M. (1991). *Acta Cryst.* A**47**, 110–119.

Keith, C., Feldman, D. S., Deganello, S., Glick, J., Ward, K. B., Jones, E. O. & Sigler, P. B. (1981). *J. Biol. Chem.* **256**, 8602–8607.

Luzzati, V. (1952). *Acta Cryst.* **5**, 802–810.

Minor, W. (1993). *XDISPLAYF Program*, Purdue University, West Lafayette, Indiana, USA.

Otwinowski, Z. (1993). *Oscillation and Data Reduction Program*, *Proceedings of the CCP4 Study Weekend: Data Collection and Processing*, edited by L. Sawyer, N. Isaacs & S. Bailey, pp. 56–62. Warrington: Daresbury Laboratory.

Perbandt, M., Wilson, J. C., Eschenburg, S., Mancheva, I., Aleksiev, B., Genov, N., Willingmann, P., Weber, W., Singh, T. P. & Betzel, C. (1997). *FEBS Lett.* **412**, 573–577.

Ramachandran, G. N. & Sasisekaran, V. (1968). *Adv. Protein Chem.* **23**, 283–438.

Scott, D. L., Mandel, A. M., Sigler, P. B. & Honig, B. (1994). *Biophys. J.* **67**, 493–504.

Scott, D. L., White, S. P., Otwinowski, Z., Yuan, W., Gelb, M. H. & Sigler, P. B. (1990). *Science*, **250**, 1541–1546.

Segelke, B. W., Nguyen, D., Chee, R., Xuong, N. H. & Dennis, E. A. (1998). *J. Mol. Biol.* **279**, 223–232.

Steiner, R. A., Rozeboom, H. J., Vries, A., Kalk, K. H., Murshudov, G. N., Wilson, K. S. & Dijkstra, B. W. (2001). *Acta Cryst.* D**57**, 516–526.

Tatulian, S. A., Biltonen, R. L. & Tamm, L. K. (1997). *J. Mol. Biol.* **268**, 809–815.

Tsai, I. H., Lu, P. J. & Su, J. C. (1996). *Toxicon*, **34**, 99–109.

Venkatachalam, C. M. (1968). *Biochim Biophys Acta*, **168**, 411–416.

Woodhams, B. J., Wilson, S. E., Xin, B. C. & Hutton, R. A. (1990). *Toxicon*, **28**, 427–433.

Yuan, W., Quinn, D. M., Sigler, P. B. & Gelb, M. H. (1990). *Biochemistry*, **29**, 6082–6094.